MANSOURA JOURNAL OF Physics
Official Journal of Faculty of Science, Mansoura University, Egypt
E-mail: scimag@mans.edu.eg ISSN: 2974-4954

Analytical versus iterative reconstruction algorithms in thyroid SPECT imaging.

Omneya M. Foda[1*].H.I.Abdel Kader[2] & H.M.Gad[3]

[1.] Physics department, faculty of Science, Mansoura University

[2.] Assistant Professor of Physics, faculty ofScience, Mansoura University.

[3.] Professor of radiodiagnosis, Urology & NephrologyCenter, faculty of Medicine, Mansoura University.

**** Correspondence to**: Omneya M. Fodaomneyafoda@gmail.comTel.: +201004647125*

Received:30/10/2021
Accepted: 14/11/2021

Abstract: In nuclear medicine SPECT has an important role in thyroid imaging. ^{99m}TC-pertechnetate was injected in patients with Graves' disease. After 20 minutes SPECT imaging was done. Projections from different angles were reconstructed to form 3D images. Analytical reconstruction algorithm, like filtered back projection (FBP), and iterative algorithms, like maximum likelihood expectation maximization (MLEM) and ordered subset expectation maximization (OSEM) were applied to improve the image physical properties: resolution, contrast and noise. After calculating the image physical parameters after reconstruction by different algorithms the conclusion was: iterative reconstruction algorithms, especially OSEM, are preferred to analytical reconstruction (FBP).

keywords: Thyroid SPECT, Reconstruction, FBP, MLEM, OSEM **.**

1.Introduction

Nuclear imaging technique is one of the most important tools for physicians to diagnose or help confirming a disease. The Gamma camera is the most familiar imaging tool in nuclear medicine to obtain a good representative image. Diagnostic imaging of the lung, brain, thyroid, heart, liver, etc. is achieved using sophisticated gamma camera with powerful software [1].

Thyroid gland is a part of the body's

endocrine system that excretes hormones which are important for regulatory functions. Nuclear medical imaging plays an important role in determining thyroid function which is helping in diagnosis, characterization or localization of many disorders. Tomography in nuclear medicine is a noninvasive imaging process that provides cross-sectional images of a three dimensional (3D) organ without superimposing tissues. There are two types of Tomography: transmission tomography like computed tomography (CT), and emission tomography like single photon emission computed tomography (SPECT). SPECT reveals the metabolic and physiological activity within an organ by providing 3D image information about the radionuclide injected into the patient. [2].

One or more rotating detectors are used in tomographic procedures to capture projections

from many different angles around the body. After that, the data is rebuilt and combined to create 3D body images. Two main methods are used to recreate tomographic images: analytical reconstruction such as filtered back projection (FBP) and iterative reconstruction such as maximum likelihood expectation maximization (MLEM) and ordered subset expectation maximization (OSEM) [3]. During image analysis after reconstruction noise appears. Noise corrupts the image quality. In order to remove the effects of noise and form a clearer picture of the actual signal, a filter is applied [4].In nuclear medicine low pass filters, such as Butterworth filter, are used to reduce noise. [5]. The criterion which we have used in judging the quality of the image is its physical parameters: resolution, contrast and noise [6].

2. SUBJECT AND METHODS

2.1 Patients.

The study was carried out in Urology and Nephrology Center in Mansoura University

after obtaining approval of Mansoura ethic community. The study included 30 patients with Graves' disease (12 male and 18 female) aged between 40-65 years.

2.2 Radiopharmaceutical

3mCi of ^{99m}Tc - pertechnetate was administered to the patients, having gamma energy of 140 keV of ^{99m}Tc and half-life of 6.02 hours. Patients were imaged after 20 minutes of injection.

2.3 Tomographic acquisitions

Dual-headed Toshiba DST-Xli gamma camera was used in this study. Each detector head housed the NaI(TL) crystal and 94 photomultiplier tubes (PMTs). SPECT tomography was applied using pinhole collimator.

The following settings were used to make tomographic acquisition: matrix size with: 128×128 pixels, pixel size 4.51×4.51 mm^2, magnification = 2. Number of views was 128 which were obtained by step and shot rotation mode of the gamma camera detector head. Time per acquisition was 20 sec. Reconstruction matrix was 128×128 pixels. Transverse slices were reconstructed.

2.4 Images Reconstruction Techniques.

2.4.1 Analytical Reconstruction

Filtered back projection algorithm (FBP)

Because of its simplicity, speed, and computing efficiency, FBP is still the most extensively utilized analytical algorithm in clinical SPECT. It includes two stages: data filtering and back projection of the data that has been filtered. Single pixel rows of the 128×128 original matrices were used to recreate transverse slices [7].

2.4.2 Iterative reconstruction

The iterative reconstruction methods involve two methods: algebraic algorithms and statistical algorithms. Statistical reconstruction includes many algorithms such as maximum likeli-hood expectation maximization (MLEM) and more advanced algorithms like ordered subset expectation maximization (OSEM) [8].

a) Maximum likelihood expectation maximization (MLEM).

An initial approximation of the image is used to begin iterative reconstruction. The iterative procedure is performed until the discrepancies between computed and measured data are less than a predetermined threshold. MLEM reconstruction was done at iteration number 2 and subset order 1.

b) Ordered Subset expectation maximization (OSEM)

To arrange projection data into an ordered series of subsets, Hudson and Larkin developed the ordered subsets EM (OSEM) [9]. Only the data in the specified subset is used to construct the MLEM projections. This approach iterates in a fraction of the time required by the traditional MLEM procedure, which uses the entire set of data perform projections. OSEM reconstruction was done at iteration number 2 and subset order 8.

2.5 Filtration

The filters used in FBP are simply mathematical equations that vary with frequency. In nuclear medicine Butterworth filter is the most common low-pass filter that is employed to reduce image noise. The critical frequency, which is the point at which the filter begins to roll-off to zero, and the order or power are the two factors that define it [5]. The order affects the filter's slope. Butterworth filter can both minimize noise and maintain image resolution due to its ability to change not just the critical frequency but also the steepness of the roll-off.

The following equation (1) describes Butterworth filter in spatial domain.

$$B(f) = \frac{1}{[1+(f/f_c)^{2n}]} \qquad (1)$$

where (f) stands for spatial frequency domain, (f_c) for critical frequency, and (n) for filter order. Butterworth filter settings used in this research were: cut-off = 0.5cm^{-1} and order 5.

2.6 Image Analysis:

The images were analyzed after reconstruction and filtering. Frame 15 of each image was analyzed for further calculations to determine image quality. Three important

parameters affect the quality of the image were calculated: resolution, contrast and noise.

Resolution

It can be expressed by the full width at half maximum (FWHM) of the line spread function (LSF) [١٠]. FWHM was calculated by drawing a vertical line profile cutting the left lobe of the thyroid and applying it in the origin-Pro(8) program in the computer, while (x –axis represent the pixels of the image ,y-axis representing the count per minute.

Contrast:

It was calculated by determining two regions of interest (ROI) in the left lobe of the imaged thyroid gland [10]. ROI size was determined to include the area of maximum activity or radiopharmaceutical in the targeted organ. Also, size of ROI on background region was set equal to that ROI on radiophar - maceutical region. Contrast was given by equation (2):

$C\%=100\times (C_{ROI} - C_{bk})/(CROI + C_{bk})$ (2)

where (C_{ROI}) is the mean counts in the ROI through the targeted area of the imaged organ and (C_{bk}) is the mean counts in the background for the same area of pixels.

Image Noise

Noise was calculated by drawing a region of interest in the left lobe of the thyroid gland [11]. The mean and standard deviation (SD) of the counts within the ROI were calculated and the percent root mean square noise (%RMS) was calculated from equation (3):

$\%RMS=100\times SD/mean$ (3)

3. RESULTS

3.1 Images

Images (with 4 frames) were collected together to represent the difference visually for the physician as shown in the following figure. Then frame 15 in each image was analyzed to evaluate resolution, contrast and noise of the image.

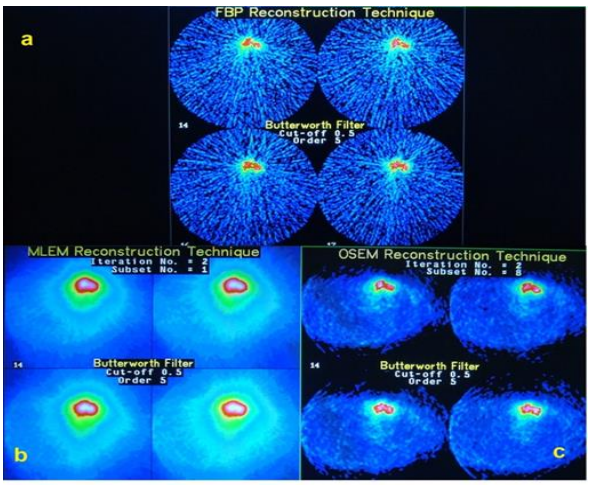

Fig.1. Transverse thyroid frames reconstructed by (a) FBP algorithm, (B) MLEM algorithm, (c) OSEM algorithm (Butterworth filter was applied with each algorithm after reconstruction).

3.2 Image Analysis

Calculating image resolution

FWHM expresses image resolution. FWHM was calculated by drawing LSP (line spread function) through origin Pro-lab8 [10]. The following figure (2) and table (1) illustrate different values of FWHM for different algorithms:

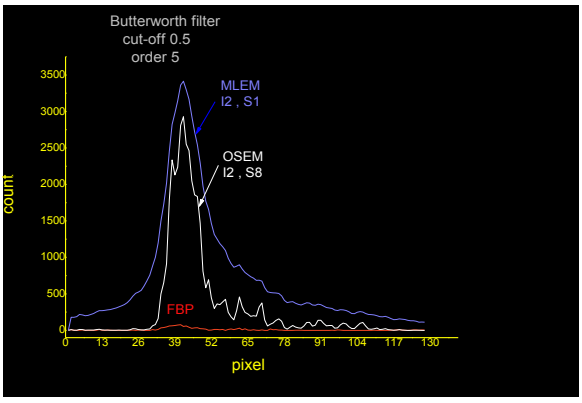

Fig.2. Three line profiles representing different values of FWHM after each algorithm of reconstruction. Different values of FWHM are shown in table (1).

Table (1) Resolution of image (FWHM) after each reconstruction algorithm.

Algorithm	FWHM (pixels)
FBP	10.42 ± 2.1
MLEM	16.89 ± 3.4
OSEM	10.77 ± 1.2

Contrast

Contrast of the image was calculated by using equation (2). The Following table shows

different values of contrast after using different reconstruction algorithms.

Table (2) Contrast of image after each reconstruction algorithm.

Algorithm	Contrast
FBP	82.73 %
MLEM	62.41 %
OSEM	86.36 %

Noise

From equation (3) percent root mean square noise (%RMS) was calculated. The Following table shows different values of (%RMS) noise after using different reconstructions algorithms.

Table (3) RMS% noise of image after each reconstruction algorithm

Algorithm	**Contrast**
FBP	37.9 %
MLEM	12.9 %
OSEM	20.7 %

Maximum Count

Maximum counts of radioactivity (counts/min) were calculated for each image after reconstruction. Maximum counts for frame 15 are shown in the following table (4).

Table (4) Maximum counts of radioactivity (counts/min) after each reconstruction algorithm.

Algorithm	**Max. Counts (counts/min)**
FBP	95
MLEM	3666
OSEM	3388

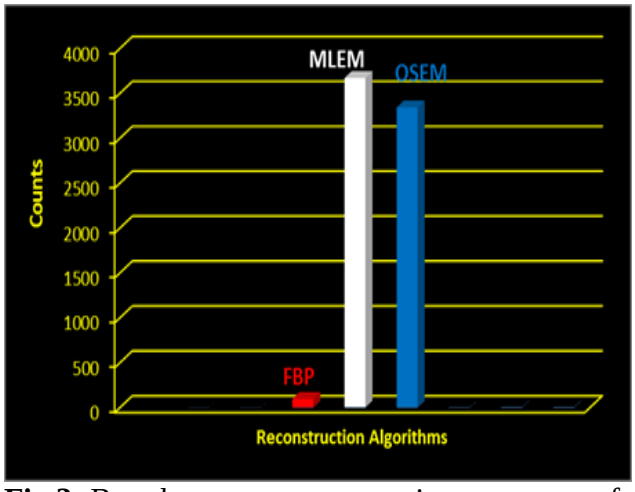

Fig.3. Bar chart represents maximum counts of radioactivity (counts/min) after each reconstruction algorithm.

4. DISCUSSION.

Figure 1 (a, b) and (c) demonstrates the results of our iteration algorithm reconstructions (MLEM & OSEM) in comparison to analytical algorithm with filtered back projection (FBP). Back projection produces more streak artifacts as shown in Figure: (1.a). FBP maintain suitable image resolution (by FWHM) of the image with suitable contrast as shown in tables (1),(2). Application of FBP algorithm eliminate many counts leading to increasing image noise, see tables (3),(4). Figure (4) shows low count rate in images reconstructed by FBP (analytical) algorithm.

The image reconstruction challenge for ECT may be thought of as a basic statistical estimation problem. When the observations may be considered as incomplete data, the expectation maximization (EM) algorithm is an iterative approach for obtaining maximum-likelihood estimations. The MLEM reconstruction methods' principal drawbacks are their sluggish convergence rate and the high computing cost of its actual implementation. [12]. From figure (1,b) we can see annular artifacts in the images reconstructed by MLEM. In this algorithm noise reduction improved on the trade- off resolution (poor resolution), see tables (2) ,(3). According to poor resolution and annular artifacts the two lobes of thyroid are overlapped and many details are diminished.

EM (OSEM) divides projection data into an ordered sequence of subsets to accelerate the image reconstruction. From figure (1.c) we can see obvious image of thyroid. Reconstruction by OSEM preserve a suitable image parameters of resolution, contrast and noise. See tables (1), (2), (3). No artifacts appeared with OSEM algorithm in our study.

The present study agreed with Eschner, W., Bähre, et.al, who used iterative reconstruction in thyroid SPECT for patients with Graves' disease [13], also agreed with Chuang, K. S., Jan, et.al, who showed that FBP is widely used in nuclear medicine because it has short reconstruction time [12].

This study also agreed with Lyra, M., & Ploussi, A., who showed that iterative reconstruction approaches result in considerable improvements in tomographic

reconstruction due to faster computerization. Iterative reconstruction methods appear to be more sensitive than the FBP algorithm in producing accurate pictures of radioactive distribution. [8].

This Study also agreed with Shin, H. B., et.al, who represented that OSEM reconst-ruction is better than FBP in noise reduction while he compared SPECT imaging with PET imaging in nuclear medicine [10].

Our study agreed with Barrack, F., Scuffham, J., et. al. who used OSEM iterative algorithm with iteration number 6 to improve diagnostic accuracy of ^{131}I imaging for patient after thyroid cancer treatment [14].

Also, our result agreed with Ben-Sellem, D. who combined Butterworth filtration with FBP, trying to optimize filter fiction for bone SPECT reconstruction, providing improved image quality and less streak artifacts. Filtration is important in FBP to reduce noise and improve image quality[15].

All SPECT processing softwares, designed to increase image quality, include both FBP and OSEM reconstruction algorithms. FBP algorithm was chosen because it was faster in terms of calculation. However, the FBP algorithm has significant problems in clinical procedures: to minimize noise, a smoothing filter is usually necessary, resulting in a loss of counts. When compared to the FBP method, the MLEM algorithm can provide improved image quality. Furthermore, the streak artifact seen when an area of the body is extremely radioactive in comparison to the background has been demonstrated to be more remarkable with FBP but reduced with MLEM algorithms. After MLEM reconstruction, annular artifacts have also been seen, particularly when the count rate is high.

5. CONCLUSION

OSEM algorithm strongly reduces many artifacts leading to best image quality in comparison with other algorithms. FBP reconstruction should be replaced with the OSEM-iterative reconstruction algorithm especially after the availability of high-performance modern computers.

6. References

1. Bushberg, J. T., & Boone, J. M. (2011). The essential physics of medical imaging Lippincott Williams & Wilkins. *ISBN* **978**-0-7817-8057-5.
2. Bruyant P.P, P. P. (2002). Analytic and iterative reconstruction algorithms in SPECT. *Journal of Nuclear Medicine*, **43(10)**, 1343-1358.
3. Zeng, G. L., (2001). Image reconstruction -a tutorial. Computerized medical imaging and graphics, **25**(2), 97-103.
4. Wendt, R. (2010). The mathematics of medical imaging: a beginner's guide. *ISBN* **978**-3-319-22664-4.
5. Khalil, M. (Ed.). Zanzonico, P. (2011). Basic sciences of nuclear medicine (pp. 155-157). M. M. Khalil (Ed.). Verlag Berlin Heidelberg: Springer. *ISBN* **978**-3-540-85961-1.
6. Gilland, D. R., Tsui, B. M., McCartney, W. H., Perry, J. R., & Berg, J. (1988). Determination of the optimum filter function for SPECT imaging. *Journal of nuclear medicine*, **29(5)**, 643-650.
7. Holly, T. A., Abbott, B. G., Al-Mallah, M., Calnon, D. A., Cohen, M. C., DiFilippo, F. P.& Soman, P. (2010). Single photon-emission computed tomography. *Journal of Nuclear Cardiology*. Volume 17, Number **5**;94173.
8. Lyra, M., & Ploussi, A. (2011). Filtering in SPECT image reconstruction. *International Journal of Biomedical Imaging.* **2011**, Article ID 693795, p. 14.
9. Hudson HM, Larkin RS. (1994). Accelerated image reconstruction using ordered subsets of projection data. *IEEE Trans Med Imaging;* **13**:601–9.
10. Shin, H. B., Kim, M. S., Law, M., Djeng, S. K., Choi, M. G., Choi, B. W. & Yoon, D. K. (2021). Application of sigmoidal optimization to reconstruct nuclear medicine image: Comparison with filtered back projection and iterative reconstruction method. *Nuclear Engineering and Technology*, **53(1),** 258-265.
11. Ackom, D., Inkoom, S., Sosu, E., & Schandorf, C. (2017). Assessment of image quality and radiation dose to adult patients undergoing computed

radiography examinations. *International journal of scientific research in science and technology*, **3(8)**, 89-94.
12. Chuang, K. S., Jan, M. L., Wu, J., Lu, J. C., Chen, S., Hsu, C. H., & Fu, Y. K. (2005) A maximum likelihood expectation maximization algorithm with thresholding. *Computerized Medical Imaging and Graphics*, **29(7)**, 571-578.
13. Eschner, W., Bähre, M., & Luig, H. (1987). Iterative reconstruction of thyroidal SPECT images. European *journal of nuclear medicine*, **13(2)**, 100-102.
14. Barrack, F., Scuffham, J., & McQuaid, S. (2018). Septal penetration correction in I-131 imaging following thyroid cancer treatment. *Physics in Medicine & Biology*, **63(7)**, 075012.
15. Ben-Sellem, D. (2021). Fast algorithm for the determination of the optimum filter for bone SPECT image reconstruction. *Research Square*, **1(24)**. ISSN 2693-5015.